Constrained optimization of active noise control systems in enclosures

T. C. Yang and C. H. Tseng
Department of Mechanical Engineering, National Chiao Tung University, Hsinchu 30050, Taiwan, Republic of China

S. F. Ling
School of Mechanical and Production Engineering, Nanyang Technological University, Singapore 2263

(Received 26 July 1993; accepted for publication 17 January 1994)

An effective software design tool is proposed for solving active noise control problems associated with constraints in which the complex strength and location of the secondary source of an active noise control system in an enclosed space are simultaneously optimized. The boundary element method is adopted to evaluate the sound field in enclosures. Furthermore, the boundary used could be of pressure, velocity, or impedance; in addition, the primary source may be at an arbitrary position. An optimizer based on sequential quadratic programming is selected for its accuracy, efficiency, and reliability. Bounds for design variables and proper constraints on the sound field and secondary source can be specified as required. The powerfulness of the proposed tool is demonstrated by optimizing an active control system for an enclosure. For a rectangular cavity, the optimal location of the secondary source is confirmed by observed simulations as always forming a dipole with the primary source situated at off-resonance excitations and subsequently approaching a mirror image position of the primary source at resonance excitations. The optimal location of the controller is found to change with varied upper bounds of the strength of the secondary source. These findings show a discrepancy from those reported in previous researches based on an unconstrained formulation. Sensitivity analysis at the optimum is also included to provide information of practical concern for implementing optimized active noise control systems.

PACS numbers: 43.50.Ki, 43.50.Jh, 43.55.Ka

INTRODUCTION

In enclosed spaces, although excellent noise control performance is attainable by passive means, such as using sound-absorbing materials, the cost becomes high and performance is significantly degraded when the acoustic wavelengths of the noise source are comparable in size with the dimensions of the enclosure, especially below Schroeder frequency.[1] Active noise control (ANC), on the other hand, is most effective in noise reduction in the relatively low-frequency range. Physically, ANC is the canceling of a sound wave by adding a phase-inversed sound wave. Methods of active noise attenuation primarily fall into two categories—reduction of the noise level in a specified region or direction[2] and reduction of total noise power.[3] The history of and recent advances in ANC are reviewed in the excellent survey papers of Warnaka,[4] Leitch and Tokhi,[5] and Stevens and Ahuja.[6]

Previous studies of optimization of ANC[7–10] in an enclosed space or exterior free space have formulated an unconstrained problem, where the optimal solutions can be analytically derived from either optimality or Kuhn–Tucker conditions.[11] However, economic factors also require consideration for practical application in the design of ANC systems in enclosures—in addition to engineering requirements, e.g., input voltage and space allowance for installation of a secondary source. Therefore, the problem of designing ANC systems in cavities via a constrained optimization model may be worthwhile.[12] Similar work on actuator placement with constraints by Clark and Fuller[13] is a suitable example for active structural acoustic control (ASAC). Once the constraints are introduced, the strategy and scheme for solving the constrained optimization problem may be relatively different from those techniques applied toward solving the unconstrained problem.

Modal summation, the finite element method (FEM), and the boundary element method (BEM) have been employed in simulating the sound field for enclosed spaces and all these methods are satisfactory predictors. The BEM can handle various kinds of boundary properties more easily than other methods, in addition to having advantages over the FEM in acoustic applications.[14] Hence, in the present study the BEM is utilized in this study for evaluating the sound field in enclosures.

A design tool that integrates the numerical acoustical analysis of BEM with an optimizer based on sequential quadratic programming (SQP) is proposed in this paper for optimizing the design of ANC systems in enclosed spaces. The complex strength (magnitude and phase) of the secondary source has normally been obtained in previous studies via the fixed position. In the present study, however, both the complex strength and location of the secondary source are simultaneously considered in the optimization formulation, which is apparently a more realistic approach to the design of ANC systems in enclosures.

 0001-4966/94/95(6)/3390/10/$6.00

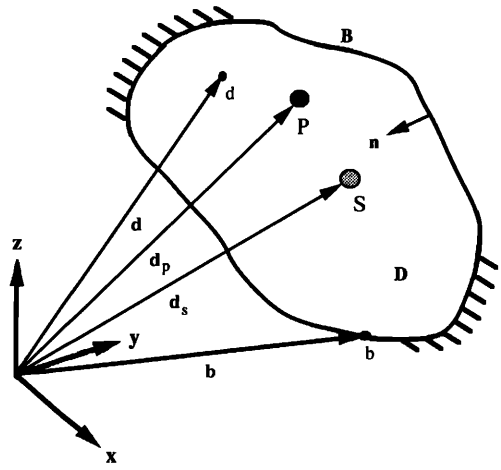

FIG. 1. Domain of acoustic system for interior Helmholtz wave equation.

The SQP is employed in this study for coping with a single-objective constrained optimization problem via a large number of design variables as a result of its robustness and fast convergence.[15–18]

The boundary element formulation of the Helmholtz equation is first discussed in this study so as to predict the sound field in enclosures. A constrained optimization model is next formulated. Achieving the characteristics of standing waves in enclosures requires choosing the total acoustic potential energy as the general objective function, like most noise control applications. Locations and strengths of secondary sources are taken as design variables in this study in light of practical considerations. Bounds on these variables and proper constraints are specified in forming a feasible design region. The usefulness and power of the proposed tool are demonstrated by numerical results on ANC optimization in a three-dimensional box cavity. A design sensitivity analysis at the optimum is finally discussed. This analysis provides the engineer with a measure of what effect such variations of an optimized ANC system designs would have on the design objective after the optimization is complete.

I. BOUNDARY ELEMENT FORMULATION IN ACOUSTICS

The acoustic system in this study consists of a domain D enclosed by a boundary B, as illustrated in Fig. 1. Vector $\mathbf{d}$ is the position of any point d within the domain; vector $\mathbf{b}$ is the boundary points b; and the location of the primary source P of complex strength ψ_p and secondary source S of complex strength ψ_s within the domain are denoted by vectors $\mathbf{d}_p$ and $\mathbf{d}_s$, respectively. The indirect BEM derived by Chen and Schweikert[19] and improved by Kipp[20] is applied in this paper to formulate the acoustical field in an interior space. The method is a numerical approximation of Huygen's principle. The boundary is assumed here to be able to be replaced by a fictitious source distribution that reproduces an identical sound field in the domain. A general form of acoustic pressure (p) and particle velocity (u) for boundary and interior points, respectively, can be written via the concept of indirect BEM as

$$p(\xi)=\int_B \sigma(b)p^*(b,\xi)dB+\int_D \psi_p(d)p^*(d,\xi)dD + \int_D \psi_s(d)p^*(d,\xi)dD, \quad (1)$$

$$u(\xi)=c_b\sigma(b)+\int_B \sigma(b)u^*(b,\xi)dB + \int_D \psi_p(d)u^*(d,\xi)dD + \int_D \psi_s(d)u^*(d,\xi)dD, \quad (2)$$

where $\sigma(b)$ represents the fictitious source density function at the boundary points, c_b is an integration constant[21] that copes with the integral singularities, and ξ is a dummy variable representing boundary or interior points. The fundamental pressure solution p^* is the free space Green's function

$$p^*(b,\xi)=(1/|b-\xi|)e^{-jk|b-\xi|}, \quad (3)$$

which satisfies

$$(\nabla^2+k^2)p^*(b,\xi)=-\delta(b-\xi), \quad (4)$$

where k is the wave number and δ is the Dirac delta function. The fundamental velocity solution u^* can be related to p^* by Euler's equation, $\rho\,\partial u/\partial t=-\nabla p$,[22] where ρ is the density of the medium.

The indirect BEM is numerically implemented by applying a linear rectangular incompatible element to discretize the boundary. The domain integral for a point sound source can be treated as a Dirac function multiplied by the source strength. Thus the integral exists only at the source point. Equations (1) and (2) are rewritten as

$$p(b_i)=\sum_{j=1}^{n_e}\int_{B_j}\sigma(b_j)p^*(b_j,b_i)dB_j + \sum_{l=1}^{n_p}\psi_{pl}p^*(d_{pl},b_i)+\sum_{m=1}^{n_s}\psi_{sm}p^*(d_{sm},b_i), \quad (5)$$

$$u(b_i)=c_b\sigma(b_i)+\sum_{j=1}^{n_e}\int_{B_j}\sigma(b_j)u^*(b_j,b_i)dB_j + \sum_{l=1}^{n_p}\psi_{pl}u^*(d_{pl},b_i)+\sum_{m=1}^{n_s}\psi_{sm}u^*(d_{sm},b_i), \quad (6)$$

where n_e, n_p, and n_s are the number of elements, primary sources, and secondary sources, respectively; B_j is the jth boundary element; and b_i represents the ith node.

Boundary conditions in terms of impedance may also be modeled via this method. For a locally reacting boundary, the specific acoustic impedance at b_i is given by[22]

$$z(b_i)=p(b_i)/u(b_i). \quad (7)$$

A system of n_e equations for the n_e unknown σ's is obtained by writing Eqs. (5), (6), and/or (7) for each

element according to the given boundary conditions. Thus the general matrix form for the equations of the system can be compactly written as

$$\mathbf{A}\sigma+\mathbf{P}\psi_{\mathbf{p}}+\mathbf{S}\psi_{\mathbf{s}}=\alpha, \tag{8}$$

where α contains the values of the boundary conditions, and **A**, **P**, and **S** can be derived from Eqs. (5), (6), or (7) according to the given boundary conditions. Once the fictitious source σ is solved, Eqs. (5) and (6) are again utilized in finding the acoustic pressure and particle velocity of domain points to be interested, in which the variable of boundary points b_i is replaced by domain points d_i.

II. CONSTRAINED OPTIMIZATION MODEL

The general mathematical model for the nonlinear single-objective constrained optimization problem considered here is of the following form.

Find a set of design variables $\mathbf{x}=(x_1,x_2,...,x_n)$ that minimizes an objective function

$$f(\mathbf{x}), \tag{9}$$

subject to the constraints

$$h_i(\mathbf{x})=0, \quad i=1,2,...,n_{\mathrm{eq}\,I}, \tag{10}$$

$$g_j(\mathbf{x})\leqslant 0, \quad j=1,2,...,n_{\mathrm{iq}\,I}, \tag{11}$$

where $n_{\mathrm{eq}\,I}$ and $n_{\mathrm{iq}\,I}$ are the number of equality and inequality constraints, respectively, and the explicit bounds on design variables are

$$x_{il}\leqslant x_i\leqslant x_{iu}, \quad i=1,2,...,n. \tag{12}$$

Both the objective function $f(\mathbf{x})$ and the constraints $h_i(\mathbf{x})$ and $g_j(\mathbf{x})$ are assumed to be continuous differentiable. The design variables **x** are the quantities to be varied for generating an optimal design. The constraints represented by Eqs. (10) and (11) define the feasible design space in conjunction with the design variable bounds specified by Eq. (12). Three elements are included in a well-defined mathematical statement of optimization—design variables, the objective function, and design constraints. The primary purpose of this study lies in forming a constrained optimization problem that optimizes the complex strength and location of the secondary source for the design of ANC systems in enclosures. Additionally, the acoustic behavior of secondary sources via appropriate constraints is also investigated.

A. Optimization strategy and formulation

As noted in the Introduction, in previous work the complex strength (for example, input voltage and phase) of the secondary source was optimized under a fixed position. In this present study, however, both location $\mathbf{d}_s$ and complex strength ψ_s of the secondary source are chosen as design variables because of practical considerations. Location $\mathbf{d}_s$ is represented here by coordinates of x, y, and z, and complex strength ψ_s is replaced by magnitude ϕ and phase θ. If the primary source is known and controlled by the secondary source, the acoustic pressure at field points of the enclosure at a given frequency can then be written as

$$p_i=p_i(x,y,z,\phi,\theta), \quad i=1,2,...,n_{\mathrm{fp}}; \tag{13}$$

where n_{fp} is the number of field points to be evaluated.

Two strategies—local and global control—can be applied where necessary. Local control implies that only a few field points of the cavity are utilized in reducing the noise level, e.g., in an automobile cabin the region near the driver's and passengers' heads is of major concern. Global control, on the other hand, is characterized by an attenuation of the noise level throughout the cavity. Each of these strategies employs an acoustic secondary source, which, for practical purposes, would typically be loudspeakers. The primary source of sound is assumed to have a harmonic waveform and can be positioned anywhere in the cavity; in addition, the secondary source can be driven at the same frequency. The position and strength of the secondary source are varied for minimizing the objective function, which is implemented in this paper by the total acoustic potential energy of the control volume. The objective function for various control strategies can always be formulated as

$$\Phi=\frac{1}{4\rho c^2}\int_V |p(x,y,z,\phi,\theta)|^2\,dV, \tag{14}$$

where c and V represent the speed of sound and the control volume, respectively. The Φ can notably be measured only by ideal distributed sensors, which may not be practical for application purposes. In practice, a reasonable number of acoustic pickups (e.g., microphones) are *uniformly distributed* throughout the cavity to collect the response utilized in formulating the discrete form of the objective function. As can be seen from Eq. (15), this form becomes very nearly proportional to the continuous form of Eq. (14) and is used in the numerical simulation. The control volume V can notably be taken out of the summation only if the error sensors are uniformly distributed throughout the cavity. Otherwise, the contribution of each sensor must be weighted:

$$\Psi=\frac{V}{4\rho c^2}\sum_{i=1}^{n_{fp}} |p_i(x,y,z,\phi,\theta)|^2. \tag{15}$$

All engineering systems are designed to perform within a given set of constraints, which includes limitations on resources, material failure, response of the system, and member sizes. Two types of constraints are introduced in this paper—design bounds and inequality constraints. Possible choices for each type of constraint are described below.

1. Bounds on design variables

The bounds are

$$x_l\leqslant x_i\leqslant x_u, \quad i=1,2,...,n_s, \tag{16}$$

$$y_l\leqslant y_i\leqslant y_u, \quad i=1,2,...,n_s, \tag{17}$$

$$z_l\leqslant z_i\leqslant z_u, \quad i=1,2,...,n_s, \tag{18}$$

$$\phi_l\leqslant \phi_i\leqslant \phi_u, \quad i=1,2,...,n_s, \tag{19}$$

$$\theta_l\leqslant \theta_i\leqslant \theta_u, \quad i=1,2,...,n_s, \tag{20}$$

where the subscripts l and u indicate the lower and upper bound of the design variables, respectively.

2. Inequality constraints

The secondary source clearly has the possibility of approaching the position of the primary source, that is, if no constraint is imposed on the relative location of the primary and secondary sources. This should be avoided in light of practical concerns. Also, for multiple control sources the spaces between the control sources must be reserved for convenient installation. Constraints of Eqs. (21) and (22), which express the permissible spaces for installing the ANC system, are therefore required from an engineering prospective:

$$\delta_{ps} - |\mathbf{d}_{pi} - \mathbf{d}_{sj}| \leqslant 0, \quad i = 1,2,...,n_p \text{ and } j = 1,2,...,n_s, \tag{21}$$

$$\delta_{ss} - |\mathbf{d}_{si} - \mathbf{d}_{sj}| \leqslant 0, \quad i = 1,2,...,n_{s-1} \text{ and } j = i+1, i+2, ..., n_s, \tag{22}$$

where δ_{ps} and δ_{ss} are the allowable distances between the primary and secondary sources, and between the secondary sources, respectively. Moreover, if the user wishes to maintain the specified sound pressure level (SPL) at particular locations; e.g., to conform to mandatory regulations, the following equation can be considered:

$$\text{SPL at } (x_j, y_j, z_j) - L_p \leqslant 0, \quad j = 1,2,...,n_{\text{spl}}; \tag{23}$$

where L_p and n_{spl} are the specified SPL and number of assigned locations, respectively.

In summary, the design optimization model presented here finds the location (x,y,z) and complex strength (ϕ,θ) of the secondary source to minimize the objective function, the total acoustic potential energy of Eq. (15), subject to the constraints of Eqs. (16)–(23).

B. Optimization scheme and algorithm

Multiple minima are basically presented in the feasible domain of the preceding optimization problem along with a number of numerical nonlinear programming (NLP) methods capable of solving it. The sequential quadratic programming (SQP) is, however, selected in this study because of its convergence and robustness.[15–18] The SQP algorithm is importantly a generalized *gradient-descent* optimization method, and subsequently converges to a local rather than global optimum.[11] A conceptual flow chart of the SQP algorithm is depicted in Fig. 2, which reflects the characteristics of the direct iterative optimization method (i.e., definition of a subproblem). This optimization method solves the subproblem to give the direction of design improvement, and a step size along the search direction. The steps of the algorithm are summarized as follows.

Step 1. Initial state: Set $k=0$. Estimate initial values of design variables as $\mathbf{x}^{(0)}$. Select an appropriate initial value for the penalty parameter $R=R_0>0$, and two small numbers that define the permissible constraint violation ϵ_1 and convergence parameter ϵ_2, respectively.

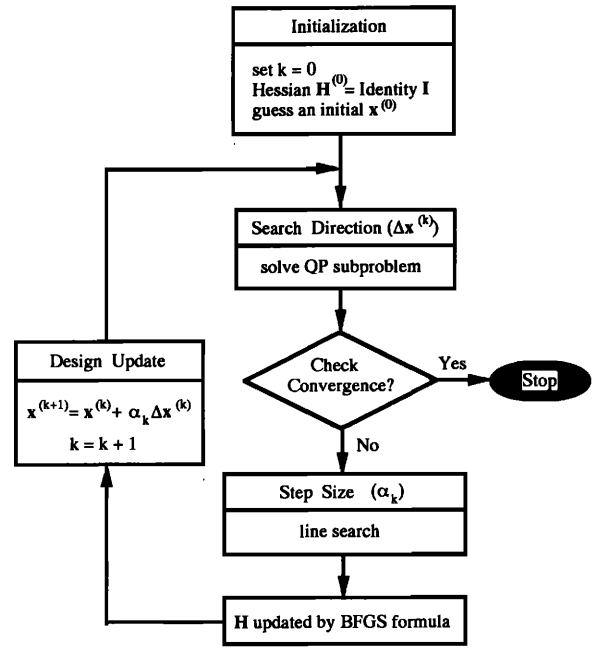

FIG. 2. Conceptual flow chart of the SQP algorithm.

Step 2. Search direction: The direction $\Delta\mathbf{x}^{(k)}$ of the iterative formula $\mathbf{x}^{(k+1)}=\mathbf{x}^{(k)}+\alpha_k\Delta\mathbf{x}^{(k)}$ is determined by solving a quadratic programming (QP) subproblem, defined as finding an n vector of $\Delta\mathbf{x}^{(k)}$ to minimize $(\nabla f(\mathbf{x}^{(k)}),\Delta\mathbf{x}^{(k)})+0.5(\Delta\mathbf{x}^{(k)},\mathbf{H}\Delta\mathbf{x}^{(k)})$, subject to the constraints $h_i(\mathbf{x}^{(k)})+(\nabla h_i(\mathbf{x}^{(k)}),\Delta\mathbf{x}^{(k)})=0$, $g_j(\mathbf{x}^{(k)})+(\nabla g_j(\mathbf{x}^{(k)}),\Delta\mathbf{x}^{(k)})\leqslant 0$, and $\mathbf{x}_{il}\leqslant\mathbf{x}^{(k)}{}_i+\Delta\mathbf{x}^{(k)}\leqslant\mathbf{x}_{iu}$, where $(A,B)=A^TB$. $\mathbf{H}$ is a positive definite approximation of the Hessian matrix, which is composed of the second partial derivatives of the Lagrangian function with respect to each of the design variables. The Lagrangian function is formed here in terms of the objective function and constraints, and is defined as $L(\mathbf{x},\mu)=f(\mathbf{x})+\Sigma\mu_i h_i(\mathbf{x})+\Sigma\mu_j g_j(\mathbf{x})$.

Step 3. Convergence criteria: If the maximum constraint violation $V(\mathbf{x}^{(k)})$ is less than a given accuracy (say, ϵ_1), and the convergence parameter $|\Delta\mathbf{x}^{(k)}|/|\nabla f(\mathbf{x}^{(k)})|$ is less than a given small number (say, ϵ_2), exit iteration. The $V(\mathbf{x})$ is defined as $\max\{0,|h_1(\mathbf{x})|,...,|h_{n'}(\mathbf{x})|,|g_{n'+1}(\mathbf{x})|,...,|h_N(\mathbf{x})|\}$, where $n' = n_{eql}$ and $N = n_{eql} + n_{iql}$.

Step 4. Penalty parameter: Calculate $r=\Sigma|\mu_i|$, where the Lagrange multipliers μ_i are obtained from the solution of the previous QP subproblem, and check the condition of $R_k\geqslant r$. If it is violated, let $R_k=2r$. Otherwise, let $R_k=R_{k-1}$. The penalty parameter R is chosen by the compromise between the constraint correction and the algorithm efficiency. The procedure applied here functions quite effectively.

Step 5. Step size: To find α_k of the iterative formula $\mathbf{x}^{(k+1)}=\mathbf{x}^{(k)}+\alpha_k\Delta\mathbf{x}^{(k)}$. A line search is used and the step size α_k is chosen as 0.5^J, with J as the smallest positive integer to satisfy the *descent* condition of $\varphi(\mathbf{x}^{(k)}+0.5^J\Delta\mathbf{x}^{(k)})\leqslant\varphi(\mathbf{x}^{(k)})-0.5^J\beta|\Delta\mathbf{x}^{(k)}|^2$, where the descent function $\varphi(\mathbf{x})=f(\mathbf{x})+RV(\mathbf{x})$ and $0<\beta<1$. The descent function is introduced because of its simplicity and

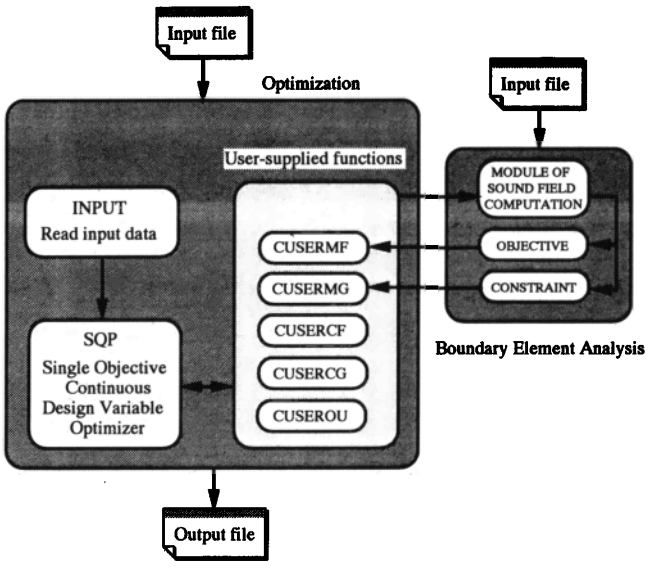

FIG. 3. Architectural framework of the proposed design tool, where CUSERXXs are user-supplied functions. CUSERMF and CUSERMG compute the value of objective and constraint functions, respectively. CUSERCF and CUSERCG calculate the gradient of objective and constraint functions, respectively. CUSEROU can provide additional data for verification.

success in solving a large number of engineering design problems.[17] Additionally, this function also has the property that its minimum value is the same as that of the original objective function.

Step 6. Hessian update: A number of procedures can be applied towards updating the Hessian matrix **H**. The BFGS (Broyden–Fletcher–Goldfard–Shanno) formula,[23,24] considered as a better strategy,[18] is selected in this paper for guaranteeing a positive definite updated Hessian. If $k=0$, let $\mathbf{H}^{(0)}$ be an identity matrix **I**.

Step 7. New iteration: Set $k=k+1$, update the design as $\mathbf{x}^{(k+1)}=\mathbf{x}^{(k)}+\alpha_k\Delta\mathbf{x}^{(k)}$, and go to Step 2.

A certain number of numerical experiences are required in implementing the scheme in terms of robustness and efficiency, despite the fact that the SQP algorithm is apparently well defined. Refer to the research of Tseng and Arora[17] for details. All the elements of the constrained optimization model defined in this paper are incorporated into an architectural framework for the proposed design tool, as exhibited in Fig. 3. The communication between the BEM acoustical analysis and the SQP optimization during the solution procedure is illustrated in this architectural framework.

III. NUMERICAL SIMULATIONS AND DISCUSSION

The active noise controllers often attempt canceling out a group of related or nonrelated harmonics during practical application by employing the same set of control sources positioned at the same locations in the cavity. Only a single harmonic line is considered in this study since this is sufficient for demonstrating the advantages afforded with the proposed optimization. In linear acoustics, however, the principle of superposition can be applied to compute the sound field. This sound field then is further utilized in forming the defined objective function and in optimizing both complex strengths and positions for the control of several harmonic lines in the proposed optimization procedure. This procedure is simply implemented by adding an iterative loop in the sound field computation module of boundary element analysis (in the right side of Fig. 3). Also, in practical applications the primary source is often outside the cavity (e.g., engine in a car or propellers in an aircraft). In coping with these applications, the appropriate analytical or measuring tool should be utilized first to investigate the impact of outside sources on the boundaries of the cavity (e.g., finding the equivalent primary sources distributed on the boundaries or inside the cavity). The BEM can accurately predict the acoustical field of the cavity if the characteristics of a boundary and/or the equivalent primary sources are well known. The primary sources are assumed here, for brevity's sake, as known and are positioned randomly anywhere in the cavity.

A geometrical configuration of a box type is most common for medium or small rooms. Consequently, the numerical simulations presented here are based on a rectangular enclosure with dimensions of 4 m×5 m×3 m. The grid points that determine the squared acoustic pressure p^2 are defined by three layers of 9×9 mesh located between $z=1.2$ m and 1.6 m (approximately the head height of a person seated in the enclosure). A frequency ranging from 30 to 200 Hz is selected to compensate for the limited accuracy of the BEM in determining the lower bound and the constraint of the Schroeder cutoff frequency for the upper bound. The primary and secondary sources are assumed here to vibrate with the same frequency and are in a steady state. For cases studied below, the acoustic system has rigid boundaries (i.e., the acoustic velocity normal to boundaries is zero).

A. Optimal location of secondary source versus frequency

No clear evidence is available in the previous literature, which indicates a specific qualitative relation between the optimal placement of the secondary source and the excitation frequency of the primary source, especially in the three-dimensional cavity. Therefore, this section is devoted to discovering such a relation. Two cases—one with single and one with multiple primary sources—are investigated. The excitation frequency of the primary source is divided into two categories—off-resonance and resonance excitations of the enclosure. For resonance excitations of the enclosure, six modes are studied: mode (0,1,0)=34.3 Hz, (1,0,0)=42.9 Hz, (0,0,1)=57.2 Hz, (0,2,0)=68.9 Hz, (2,0,0)=86.1 Hz, and (2,2,0)=110.6 Hz. Typical results obtained for these cases are discussed below.

1. Enclosure with single primary source

A primary source P_1 of volume velocity 1 m^3/s is positioned close to one corner (3.8,4.5,2.5) of the cavity with a harmonic excitation. The design bounds and constraints, respectively, are $0\leqslant\phi_s\leqslant 1$ m^3/s, $-180\leqslant\theta_s\leqslant 180$ deg, $0\leqslant x\leqslant 4$ m, $0\leqslant y\leqslant 5$ m, $0\leqslant z\leqslant 3$ m, 0.1 m$\leqslant|\mathbf{d}_p-\mathbf{d}_s|$, and SPL at (1.5,1.2,1.4) and (3.2,4,1.6)$\leqslant$100 dB, which are arbi-

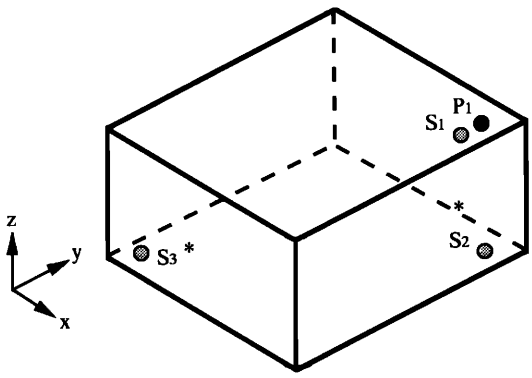

FIG. 4. Schematic diagram of ANC in the enclosure with single primary source. Primary source P_1 is positioned at (3.8,4.5,2.5). Optimal candidate locations of secondary source are as follows: $S_1=(3.8,4.4,2.5)$, $S_2=(3.8,4.5,0.5)$, and $S_3=(0.2,0.5,0.5)$. The asterisk represents the position of specified SPL.

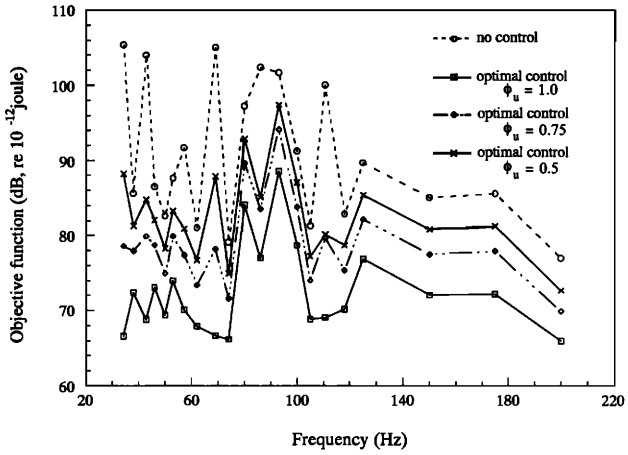

FIG. 5. Objective function as a function of frequency for the case of rectangular enclosure with single primary source (Secs. III A 1 and III B). ϕ_u is the upper bound of the strength of the secondary source.

trarily chosen for illustrative purposes. At off-resonances, the optimal secondary source always approaches closely a position of $S_1=(3.8,4.4,2.5)$ with an antiphase (i.e., -180 deg), where it approximately forms a dipole with the primary source P_1. For a cavity of simple geometrical configuration (e.g., the rectangular one used in this paper), the position of *maximum* acoustic pressure (globally) is primarily located in the vicinity of the primary source at off-resonance excitations. Via this simple geometrical constraint, the optimal secondary source positioned in or close to this place can effectively attenuate the noise as indicated by the above results. More than one position of *peak* acoustic pressure (locally) is available in the cavity at higher excitation frequencies of the primary source [but still below the Schroeder cutoff frequency (in this example 200 Hz)]. The solution can therefore be varied from different initial designs in light of the algorithm searching for the local minimum. The optimization solutions shown here and after are selected from the better one of various initial conditions. However, a totally different situation is obtained at resonances of the enclosure. The optimal secondary source of modes (0,1,0), (1,0,0), and (2,0,0) approaches $S_2=(3.8,4.5,0.5)$, a *mirror image* position of P_1 along an *edge*, and it approaches $S_3=(0.2,0.5,0.5)$, a *mirror image* position of P_1 along a *diagonal*, for modes of (0,2,0) and (2,2,0). The optimal secondary source is, however, patched to $S_1=(3.8,4.4,2.5)$ for mode (0,0,1). Physically, the results for a cavity with a simple geometrical configuration can be related to the position of the primary source, and the shape of sound field in the enclosure, in which it is almost of geometrical symmetry and the positions of peak acoustic pressure are close to the boundaries. The relative positions of P_1, S_1, S_2, and S_3 are shown in Fig. 4. The complex strength of the optimal secondary source in each case is of volume velocity 1 m^3/s and phase -180 deg shift relative to the primary source. This knowledge of the distribution of the optimal secondary source in the frequency range of interest suggests that a sufficient guideline for setting up an ANC system lies in either attempting an *edge* or *diagonal mirror image* position of the primary source for resonance excitation or placing the secondary source *close to* the primary source for off-resonance excitation. The mirror image strategy is similar to that of efficient coupling into the appropriate mode, as advocated by Bullmore *et al.*[25] in a two-dimensional cavity, in which the placement of the secondary source is based on the shape analysis of sound field before control. However, for cavities of irregular boundaries it is not easy to predict the positions of peak acoustic pressures in advance. Therefore, an optimization procedure optimizing the positions and complex strengths of the control sources at the same time makes the tool very attractive for practical work in active noise control. Note that this rule is generally valid for simple cavities with geometrical constraints among the sound sources. Figure 5 illustrates that the optimal controller performs well at frequencies below 100 Hz, where reduction of total acoustic potential energy is more than 15 dB. All of the constraints are satisfied in these simulations and the SPL at the specified positions is below 90 dB, which implies that this constraint is inactive.

2. Enclosure with multiple primary sources

Two primary sources, P_1 and P_2 of volume velocity 1 m^3/s, in-phase, and the same excitation frequency, are positioned close to (3.8,4.5,2.5) and (0.2,2.5,1.5), respectively. The *one-on-one* approach is chosen as the control technique that attenuates the noise level in a specified region; that is, each primary source is controlled by a corresponding secondary source. The design bounds are $0\leqslant\phi_{s1},\phi_{s2}\leqslant 1$ m^3/s, $-180\leqslant\theta_{s1},\theta_{s2}\leqslant 180$ deg, $0\leqslant x_1,x_2\leqslant 4$ m, $0\leqslant y_1,y_2\leqslant 5$ m, and $0\leqslant z_1,z_2\leqslant 3$ m, and the constraints are $0.1\text{ m}\leqslant|\mathbf{d}_{p1}-\mathbf{d}_{s1}|$, $0.1\text{ m}\leqslant|\mathbf{d}_{p1}-\mathbf{d}_{s2}|$, $0.1\text{ m}\leqslant|\mathbf{d}_{p2}-\mathbf{d}_{s1}|$, $0.1\text{ m}\leqslant|\mathbf{d}_{p2}-\mathbf{d}_{s2}|$, $0.1\text{ m}\leqslant|\mathbf{d}_{s1}-\mathbf{d}_{s2}|$, and SPL at positions of (1.5,1.2,1.4) and (3.2,4,1.6)$\leqslant$100 dB, respectively.

At resonance excitations of the enclosure, the optimal locations of the secondary sources are at $S_1=(3.8,4.5,0.5)$ and $S_2=(3.8,2.5,1.5)$ for modes of (0,1,0) and (2,0,0); meanwhile, for other modes they change to $S_3=(3.8,4.4,2.5)$ and $S_4=(0.2,2.5,1.6)$. Relative positions

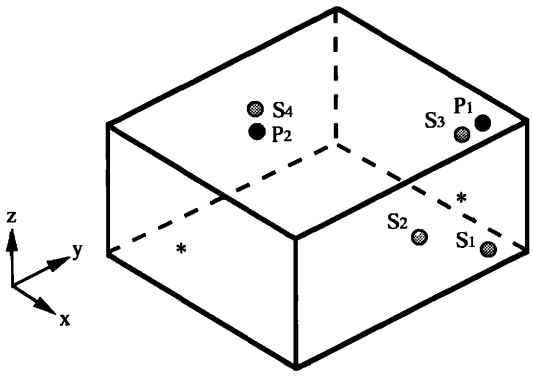

FIG. 6. Schematic diagram of ANC in the enclosure with multiple primary sources. Locations of primary sources P_1 and P_2 are positioned at (3.8,4.5,2.5) and (0.2,2.5,1.5), respectively. Optimal candidate locations of secondary sources are as follows: $S_1=(3.8,4.5,0.5)$, $S_2=3.8,2.5,1.5)$, $S_3=(3.8,4.4,2.5)$, and $S_4=(0.2,2.5,1.6)$. The asterisk represents the position of specified SPL.

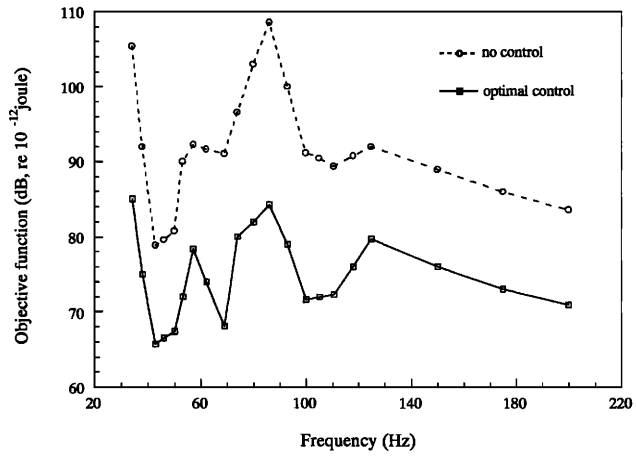

FIG. 7. Objective function as a function of frequency for the case of rectangular enclosure with multiple primary sources (Sec. III A 2).

of S_1, S_2, S_3, and S_4 are shown in Fig. 6. The optimal complex strength for all the secondary sources is 1 m^3/s in magnitude and -180 deg in phase shift. Note that at resonance excitations, the optimal locations of the secondary sources are primarily not at edge or diagonal mirror image positions of the primary sources. However, these locations tend to form a dipole with the corresponding primary source. At off-resonance excitations, the optimal locations of the secondary sources are always at S_3 and S_4, respectively, where they tend to form a dipole with the corresponding primary source. The same physical reasoning as in Sec. III A 1 can be applied on the basis of the above results. For the case of multiple primary sources, however, the sound field in the enclosure is more complex than the one of a single primary source. Additionally, its locations of maximum and/or peak acoustic pressure are highly dependent on the relative positions and phase differences of the primary sources. Unlike the case of a single primary source, predicting the optimal locations of the controllers would be difficult without carrying out simulations such as those described here. However, a general strategy for the placement of secondary sources for the case of multiple primary sources can still be suggested. The secondary source is first patched so as to form a *dipole* with the corresponding primary source. If that does not work, one should then attempt to position the secondary source in an *edge mirror* position of the corresponding primary source. This is somewhat different from the strategy demonstrated in Sec. III A 1. The performance of the optimal ANC is verified in Fig. 7 by the reduction of the total acoustic potential energy in the control volume, where it is over 15 dB in the frequency below 110 Hz.

B. Effect of design bound ϕ_u

Table I compares the optimal locations of the secondary source at resonance excitations of the enclosure for different upper bounds on the strength of the secondary source, ϕ_u. The enclosure of a single primary source is again discussed here, assuming that the volume velocity of the primary source is 1 m^3/s. As expected, for the case where $\phi_u > 1$ m^3/s the optimal placement of the secondary source is the same as that for the case where $\phi_u = 1$ m^3/s. This is because for cavities of simple geometrical configuration the primary and secondary source having equal but inverse contribution can make the greatest noise reduction in a one-on-one control strategy.

For cases of $\phi_u < 1$ m^3/s, however, the location of the optimal controller is quite different from that in the case of $\phi_u = 1$ m^3/s. Because of the lack of effective power, in most situations the controller cannot be afforded with the largest attenuation at the position of the case $\phi_u \geqslant 1$ m^3/s; as a result, the controller converges to the other place (local minimum) by tailoring its strength. As mentioned in Sec. III A, the positions of peak acoustic pressure are in or close to the boundaries of the cavity at resonance excitations. Hence, for the case of $\phi_u < 1$ m^3/s the optimal location of the secondary source is definitely in the vicinity of the mirror image of the primary source. For $\phi_u < 1$ m^3/s the optimal location would generally approach a position some distance away from an edge or a diagonal mirror image position of the primary source. Furthermore, the objective function increases as ϕ_u decreases. For example, at 34.3 Hz the optimal locations of the secondary source for $\phi_u \geqslant 1$, $\phi_u = 0.75$, and $\phi_u = 0.5$ m^3/s are at (3.8,4.5,0.5), $(0.2,0.5,2.5)^+$, and $(0.2,0.5,0.5)^+$, respectively, where the superscript "+" indicates "in the neighborhood of." At resonances of 68.9 and 110.6 Hz, however, the optimal controller of $\phi_u < 1$ m^3/s is located in the vicinity of the position of $\phi_u \geqslant 1$ m^3/s along with the values of the objective function for $\phi_u \geqslant 1$ m^3/s and $\phi_u = 0.75$ m^3/s being quite close (at least in the first decimal digit). This infers that for $\phi_u \geqslant 0.75$ m^3/s at these two resonances, the objective function is insensitive to the variation of design variables in the neighborhood of the position (0.2,0.5,0.5).

The upper bound of the strength of the secondary source having a definite impact on the optimal placement of the controller is confirmed by the above results. Also, at the optimum the magnitude ϕ of the secondary source reaches to ϕ_u in most situations, where only maximum

TABLE I. Comparison of the optimal location of the secondary source with objective function at resonances of the enclosure for various upper bounds on the strength of the secondary source, ϕ_u. The superscript "+" indicates "in the neighborhood of."

Frequency (Hz)	ϕ_u>1 m^3/s		ϕ_u=0.75 m^3/s		ϕ_u=0.5 m^3/s		No control
	(x,y,z)	f (dB)	(x,y,z)	f (dB)	(x,y,z)	f (dB)	f (dB)
34.3	(3.8,4.5,0.5)	65.3	(0.2,0.5,2.5)$^+$	78.6	(0.2,0.5,0.5)$^+$	88.2	105.4
42.9	(3.8,4.5,0.5)	67.5	(0.2,0.5,2.5)$^+$	79.9	(3.8,0.5,0.5)$^+$	84.8	103.6
57.2	(3.8,4.4,2.5)	77.4	(0.2,4.5,0.5)$^+$	78.3	(0.2,0.5,2.5)$^+$	80.9	92.4
68.9	(0.2,0.5,0.5)	78.2	(0.2,0.5,0.5)$^+$	78.2	(0.2,0.5,0.5)$^+$	87.9	105.1
86.1	(3.8,4.5,0.5)	77.0	(3.8,0.5,0.5)$^+$	83.6	(0.2,0.5,0.5)$^+$	85.1	102.4
110.6	(0.2,0.5,0.5)	79.6	(0.2,0.5,0.5)$^+$	79.6	(0.2,0.5,0.5)$^+$	80.1	99.9

output of the controller can make the effective noise reduction. The optimal phase θ is normally either a 0 or -180 deg shift, which depends on the phase of the optimal position in the sound field before control, relative to the primary source. From a practical point of view, the general strategy for placement of the optimal controller obtained in Sec. III A must be modified if the power of the secondary source being smaller than that of the primary source is used.

IV. SENSITIVITY ANALYSIS

Two categories of sensitivity information are generally of interest and significance during and/or after optimization of engineering systems. Parameter sensitivity analysis is to be performed if system parameters are modified after the optimization is complete. The primary objective of parameter analysis lies in both estimating the sensitivity of an optimum design to some new problem parameter and providing the engineer with a measure of what effect such changes would have on the design. Some useful methods, including the traditional approach based on the Kuhn–Tucker necessary conditions for optimality, are available in Vanderplaats and Yoshida.[26] A systematic sensitivity analysis using a multiobjective optimization approach for the determination of system parameters has also recently been proposed.[27] Another kind of sensitivity information is the first and second derivatives of objective and constraint functions on design variables, which are also referred to as the gradient and Hessian, respectively. Such information plays a key role in the search of optimal point. Most search methods require either first- or second-order information. Deriving an explicit expression for gradient and Hessian is often difficult in an engineering design optimization as a consequence of the complexity of engineering systems. Therefore, how this information can be accurately and efficiently obtained has been extensively investigated.[28] One simple but extensively utilized approach is the finite difference method. For a given tolerance, this approach can provide an adequate approximation to either first- or second-order derivatives.

The estimation of effects of relative small errors present during the installation and/or operation of the optimal controller on the optimal design is of primary concern in this study. Therefore, the sensitivity of objective function on design variables, i.e., position vector for installation and complex strength for operation, can be practical for required sensitivity analysis. A case of Sec. III A 1 is employed in demonstrating the concept of sensitivity analysis described above. The required sensitivity $\partial f(\mathbf{x})/\partial \mathbf{x}$ for design variables $\mathbf{x}$ is shown in Fig. 8 at various frequencies, in which it is divided into three groups because of different dimensions for design variables. Table II is included to compensate for any misconception that has probably arisen from the fact that the sensitivity to position (x, y, and z) actually has not the same dimensions as that for strength (ϕ and θ). The effect of each design variable on the design objective is presented in Table II under a specified variation of the optimal value. Via this information, more attention is drawn to those design variables that have a significant effect on design requirement in the course of installation and operation. As a result, the required optimum design can be correctly implemented. On the other hand, the total resulting variation of objective function can be evaluated on the basis of the deviations of design variables $\delta\mathbf{x}$ (after final setting up) by $\delta f = \partial f/\partial x_1\,\delta x_1 + \partial f/\partial x_2\,\delta x_2 + \cdots + \partial f/\partial x_n\,\delta x_n$. An optimal configuration is assumed to be reached if this value is within an acceptable range; otherwise, retuning of the controller is necessary. Some conclusions can be drawn from the sensitivity information and the effect of each design variable on the objective function given in Fig. 8 and Table II.

(i) For position components, the sensitivity with respect to x is generally more significant with all resonant frequencies. This implies that the x component of the position of the controller demands more accuracy during in-

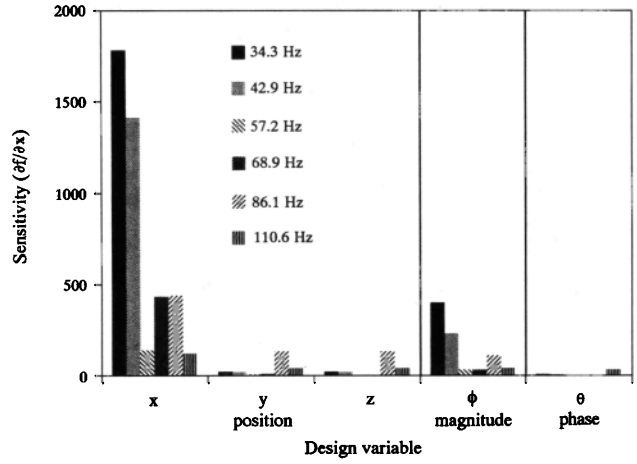

FIG. 8. Sensitivity analysis of the secondary source at optimum.

TABLE II. The effect of a small variation of design varables on the objective function at the optimum. The figures provided here represent the increase of objective function in decibels. Note that while one of design variables is varied, the other variables remain unchanged.

	Frequency (Hz)					
Variation	34.3	42.9	57.2	68.9	86.1	110.6
$\delta x=0.01$ m	17.77	14.09	1.43	4.29	4.42	1.22
$\delta y=0.01$ m	0.22	0.20	1.20	0.03	1.31	0.02
$\delta z=0.01$ m	0.17	0.24	0.01	0.01	1.31	0.03
$\delta\phi=0.01$ m^3/s	4.04	2.68	0.32	0.27	1.07	0.12
$\delta\theta=1$ deg	6.66	4.08	0.02	0.20	0.69	0.38

stallation while others may allow some deviations. However, the x dominate can be related to the *shape of sound field* in this *simple* cavity. At resonance excitations, the shape of original sound field in the vicinity of the mirror image of the primary source (such as the positions of S_2 and S_3 in Fig. 4) is quite *flat* along the y or z direction but rather *steep* along the x direction, especially at resonances of 34.3 and 42.9 Hz. Hence, a small variation of δx with the optimal value has a larger effect than those of δy and δz on the objective function. Also, the effect of variation δx at lower frequencies of 34.3 and 42.9 Hz is more crucial than that at higher frequencies, where reasoning similar to that above can be applied.

(ii) For the characteristics of the controller itself, the given sensitivity indicates that the design objective is generally insensitive to the variation of $\delta\phi$ (except for 34.3 and 42.9 Hz) and $\delta\theta$. This sensitivity arises since the optimal placement of the secondary source is of efficient coupling into the appropriate mode, in which the design objective is primarily influenced by the positions of peak acoustic pressure (local minima). In light of the different dimensions of ϕ and θ, the combination of sensitivity analysis (Fig. 8) and the effect of design variable on the objective (Table II) is required for evaluating their influence. For example, at resonance of 34.3 Hz the sensitivity of $\partial f(\mathbf{x})/\partial\mathbf{x}$ for ϕ is substantially larger than that for θ. From Table II, a variation of $\delta\phi=0.01$ m^3/s produces a 4.04-dB increase of objective function and, however, a 6.66-dB increase for the variation of $\delta\theta=1$ deg. Further, if the variation is doubled, a 7.85-dB increase of objective function would occur for $\delta\phi=0.02$ m^3/s, as compared to a 11.66-dB increase for $\delta\theta=2$ deg. Accurately controlling the phase of controller is difficult in application. From this point of view and the results shown above, careful tuning is thus required in setting up the phase of the controller.

(iii) The sensitivity with respect to $\mathbf{x}$ at 57.2 Hz is significantly less than that at other frequencies. In this case, the objective function is apparently insensitive with respect to all design variables. However, which factor will dominate the design? The optimal location of the secondary source in this case can be postulated as being so close to the primary source that the former can still produce the proper approximated inversed acoustic field so as to attenuate the noise under a small variation of $\delta\mathbf{x}$. This argument is supported by the observation that the inequality constraint, which defines the allowable distance between the primary and secondary sources, is active in this case. Further insight into the sensitivity on the constraint could be obtained by performing a parameter sensitivity analysis with respect to parameter δa, i.e., the inequality constraint is changed from $g(\mathbf{x})\leqslant 0$ to $g(\mathbf{x})\leqslant\delta a$. The multiobjective optimization approach reported by Tseng and Lu[27] is suggested for further details regarding the sensitivity on δa.

A working instruction on the installation and operation of the active noise control system can be drawn on the basis of the optimal design along with the above sensitivity analysis so as to guide all of the implementations.

V. CONCLUDING REMARKS

An effective software design tool was proposed in this study for solving active noise control problems associated with constraints, in which the complex strength and location of the secondary source of an active noise control system in an enclosed space are simultaneously optimized. In light of practical considerations, the design of an active noise control system in an enclosure was formulated as a constrained optimization problem but not as an unconstrained one as proposed in previous research efforts. The approach presented above was found to be straightforward and versatile. The acoustic properties of the enclosure boundaries and the complex strength and location of the primary and secondary sources could easily be varied. The parameters assigned in the optimization scheme SQP proved effective in ensuring the scheme robust as it converges quickly (within a few iterations) for all the example cases. Convergence to a local minimum would also be guaranteed by this scheme for various initial designs.

This constrained optimization model was applied toward designing ANC systems for a rectangular cavity through computer simulations. Results indicated the optimal location of the secondary source generally tends to form a dipole with the primary source at off-resonance excitations and approaches a mirror image position of the primary source at resonance excitations of the enclosure. Furthermore, the optimal location of the controller was observed to change for varied rates of output powers of the secondary source, which corresponds to the upper bound of the strength of the secondary source. The effect of a small variation in δx being crucial was confirmed by sensitivity analysis at the optimum, especially at lower resonant frequencies. Consequently, this effect could be related to the shape of sound field in this simple cavity.

ACKNOWLEDGMENTS

The authors acknowledge the support of the National Science Council, Taiwan, R.O.C., under Grant No. NSC82-0401-E009-085. Review of this manuscript by T. W. Lu is also appreciated.

[1] T. Salava, "Acoustic load and transfer functions in rooms at low frequencies," J. Audio Eng. Soc. **36**, 763–775 (1988).

[2] S. Onoda and K. Kido, "Automatic control of stationary noise by means of directivity synthesis," Proc. 6th ICA Congr. Tokyo **IV**, F185–188 (1968).

[3] P. A. Nelson, A. R. D. Curtis, S. J. Elliott, and A. J. Bullmore, "The minimum power output of free field point sources and the active control of sound," J. Sound Vib. **116**, 397–414 (1987).

[4] G. E. Warnaka, "Active attenuation of noise—The state of the art," 1982 Noise Contr. Eng. J. **18**, 100–110 (1982).

[5] R. R. Leitch and M. O. Tokhi, "Active noise control systems," IEE Proc. A **134**, 525–546 (1987).

[6] J. C. Stevens and K. K. Ahuja, "Recent advances in active noise control," AIAA J. **29**, 1058–1067 (1991).

[7] P. A. Nelson, A. R. D. Curtis, S. J. Elliott, and A. J. Bullmore, "The active minimization of harmonic enclosed sound fields, part I: Theory," J. Sound Vib. **117**, 1–13 (1987).

[8] C. G. Mollo, "A numerical method for analyzing the optimal performance of active noise controller," M.Sc. thesis, Purdue University (1987).

[9] K. A. Cunefare and G. H. Koopmann, "A boundary element approach to optimization of active noise control sources on three-dimensional structures," J. Vib. Acoust. **113**, 387–394 (1991).

[10] C. H. Jo and S. J. Elliott, "Active control of low frequency sound transmission between rooms," J. Acoust. Soc. Am. **92**, 1461–1472 (1992).

[11] J. S. Arora, *Introduction to Optimum Design* (McGraw-Hill, New York, 1989).

[12] T. C. Yang, C. H. Tseng and B. T. Lee, "A Boundary Element and Optimization Approach for Designing of Active Noise Control Systems in Enclosures," Proc. Int. Noise Vib. Contr. Conf., St. Petersburg, Russia, **3**, 269–274 (1993).

[13] R. L. Clark and C. R. Fuller, "Optimal placement of piezoelectric actuators and polyvinylidence fluoride error sensors in active structural acoustic control approaches," J. Acoust. Soc. Am. **92**, 1521–1533 (1992).

[14] P. K. Banerjee and R. Butterfield, *Boundary Element Methods in Engineering Science* (McGraw-Hill, London, 1981).

[15] K. Schittkowski, "The nonlinear programming method of Wilson, Han and Powell with an augmented Lagrangian type line search function, part I: Convergence analysis; Part II: An efficient implementation with linear least squares subproblem," Num. Meth. **38**, 83–127 (1981).

[16] J. Stoer, "Foundations of recursive quadratic programming methods for solving nonlinear programs," in *Proceedings of the NATO Advanced Study Institute on Computational Mathematical Programming*, Bad Windshim, Germany (1984).

[17] C. H. Tseng and J. S. Arora, "On implementation of computational algorithms for optimal design, part I: Preliminary investigation; Part II: Extensive numerical investigation," Int. J. Num. Meth. Eng. **26**, 1365–1402 (1988).

[18] C. H. Tseng and W. C. Liao, "Integrated software for multifunction optimization," M.Sc. thesis, National Chiao Tung University, R.O.C. (1990).

[19] L. H. Chen and D. G. Schweikert, "Sound radiation from an arbitrary body," J. Acoust. Soc. Am. **35**, 1626–1632 (1963).

[20] C. R. Kipp, "Prediction of sound fields in acoustical cavities using the boundary element method," M.Sc. thesis, Purdue University (1985).

[21] C. A. Brebbia and S. Walker, *Boundary Element Techniques in Engineering* (Newnes-Butterworths, London, 1980).

[22] L. E. Kinsler, A. R. Frey, A. B. Coppens, and J. V. Sanders, *Fundamentals of Acoustics* (Wiley, New York, 1982).

[23] M. J. D. Powell, "The convergence of variable metric methods for nonlinearly constrained optimization calculations," in *Nonlinear Programming*, Vol. 3, edited by O. L. Mangasarian *et al.* (Academic, New York, 1978).

[24] P. B. Thanedar, J. S. Arora, and C. H. Tseng, "A hybrid optimization method and its role in computer-aided design," Comp. Struct. **23**, 305–314 (1986).

[25] A. J. Bullmore, P. A. Nelson, A. R. D. Curtis, and S. J. Elliott, "The active minimization of harmonic enclosed sound fields, part II: A computer simulation," J. Sound Vib. **117**, 15–33 (1987).

[26] G. N. Vanderplaats and N. Yoshida, "Efficient calculation of optimum design sensitivity," AIAA J. **23**, 1798–1803 (1985).

[27] C. H. Tseng and T. W. Lu, "Minimax multiobjective optimization in structural design," Int. J. Num. Meth. Eng. **30**, 1213–1228 (1990).

[28] C. H. Tseng and K. Y. Kao, "Performance of a hybrid design sensitivity analysis on structural design problems," Comp. Struct. **33**, 1125–1131 (1989).